

1 Proceedings

2 Water Budgets of Tropical Cyclones Through a 3 Lagrangian Approach: A Case of Study of Hurricane 4 Irma (2017)

5 Albenis Pérez-Alarcón^{1,2,*}, Raquel Nieto¹, Luis Gimeno¹, José C. Fernández-Alvarez^{1,2}; Patricia Coll-Hidalgo^{1,4} and
6 Rogert Sorí^{1,3}

7 ¹ Centro de Investigación Mariña, Universidade de Vigo, Environmental Physics Laboratory (EPhysLab),
8 Campus As Lagoas s/n, Ourense, 32004, Spain; albenis.perez.alarcon@uvigo.es (A.P.-A.); rnieto@uvigo.es
9 (R.N.); l.gimeno@uvigo.es (L.G.); rogert.sori@uvigo.es (R.S.); jose.carlos.fernandez.alvarez@uvigo.es (J.C.F.-
10 A.); patricia.coll (P.C.-H.)

11 ² Departamento de Meteorología, Instituto Superior de Tecnologías y Ciencias Aplicadas, Universidad de La
12 Habana, 10400, La Habana, Cuba

13 ³ Instituto Dom Luiz, Faculdade de Ciências da Universidade de Lisboa, 1749-016 Campo Grande, Portugal

14 ⁴ Empresa Cubana de Navegación Aérea, 10400 La Habana, Cuba

15 * Correspondence: albenis.perez.alarcon@uvigo.es (A.P.-A.)

16 **Abstract:** This study examined the water budget of Hurricane Irma (2017) through a Lagrangian
17 approach. To identify the moisture sources for the Hurricane Irma genesis and intensification the
18 particle dispersion model FLEXPART was used. The North Atlantic Ocean between 15° and 30°
19 North latitude and the South Atlantic Ocean were identified as the main moisture sources for Irma
20 development. From the perspective of the water budget, the maximum accumulated precipitation
21 along Irma's trajectory coincides with the maximum water budget efficiency, which suggests that
22 total precipitation depends largely on the water vapour supplied, rather than the storm intensity.
23 Furthermore, the moisture supplies from the surface under the area delimited by hurricane size is
24 small, thus, the water vapour supplies from the environment through the secondary circulation
25 transports more moisture inward.

26 **Citation:** Pérez-Alarcón, A.; Nieto,
27 R.; Gimeno, L.; Fernández-Alvarez,
J.C.; Coll-Hidalgo, P.; Sorí, R. Water
Budgets of Tropical Cyclones

28 Through a Lagrangian Approach: A
29 Case of Study of Hurricane Irma
30 (2017). *Proceedings* **2021**, *65*, x.
31 <https://doi.org/10.3390/xxxxx>

32 Received: date

33 Accepted: date

34 Published: date

35 **Publisher's Note:** MDPI stays
36 neutral with regard to jurisdictional
37 claims in published maps and
38 institutional affiliations.



41 **Copyright:** © 2021 by the authors.
42 Submitted for possible open access
43 publication under the terms and
44 conditions of the Creative Commons
Attribution (CC BY) license (<http://creativecommons.org/licenses/by/4.0/>).

Keywords: tropical cyclones; water budget; moisture transport; precipitation

1. Introduction

Tropical cyclones (TCs) are one of the natural hazards that annually cause major disasters worldwide, including many human deaths and large economic losses due to the increasing populations in coastal regions and the increasing economic value of infrastructures [1].

Among others factors, TCs formation requires moist layers at mid-troposphere to enhance thunderstorm formation [2,3]. Thus, the cyclone scale circulation provides moisture for cumulus development, and the latent heat release in cumulus clouds drives the cyclone circulation in return. Several author [4-10] have investigate the role of the atmospheric humidity in TC development. There are several methods to investigate the origin of moisture (e.g., Eulerian, and Lagrangian). A further review and comparison of the different approaches used to study moisture transport may be found in Gimeno et al. [11].

Although there have been many observational and modeling studies of TCs, and the Lagrangian diagnostic scheme has proved to be a powerful tool to identified moisture sources and study anomalous atmospheric moisture transports [12,13], the TCs' water budgets through a Lagrangian approach has been poorly studied. Thus, in this study we

45 aim to investigate the water budget of North Atlantic Hurricane Irma (2017) using the
46 Lagrangian analysis

47 *1.1 Hurricane Irma (2017)*

48 The Hurricane Irma (2017) was formed from a tropical wave at 0000 UTC 30 August
49 [32]. While moving westward to the south of a mid-level ridge over the eastern Atlantic,
50 Irma strengthened rapidly in environmental conditions of low vertical wind shear and a
51 fairly moist lower troposphere while it was over marginally warm sea surface
52 temperature (SST). Only 48 h after genesis, Irma reached the major hurricane strength
53 (category +3 hurricane on Saffir – Simpson scale) at 0000 UTC 1st September. The RI
54 process (130 km/h in 48 h) undergone by Irma is a remarkable rate that has only achieved
55 by a small fraction of Atlantic tropical cyclones [14].

56 The hurricane reached its maximum intensity of 286 km/h around 1800 UTC 5
57 September. As a category 5 hurricane, Irma made landfall on Barbuda and St. Martin
58 around 0545 UTC and 1115 UTC 6 September, respectively. About 1630 UTC 6
59 September Hurricane Irma made its third landfall on the island of Virgin Gorda in the
60 British Virgin Islands as category 5 hurricane [14]. Irma again made landfall on Little
61 Inagua Island in the Bahamas at 0500 UTC 8 September category 4 intensity. Irma then
62 turned slightly to the left, due to a building subtropical ridge, and moved toward the
63 northern coast of Cuba and made the fifth landfall near Cayo Romano, Cuba, at 0300
64 UTC 9 September, with estimated maximum winds of 270 km/h.

65 The land interaction of the storm circulation in its movement along the northern
66 coast of Cuba led to Irma weakening to a category 2 hurricane, however, the movement
67 over warm waters in the Straits of Florida allowed that the hurricane re-intensified once
68 again before making landfall for the sixth time near Cudjoe Key in the lower Florida
69 Keys around 1300 UTC 10 September [14]. Finally, Irma dissipated at 1200 UTC 13
70 September.

71 **2. Material and Methods**

72 *2.1 Data*

73 The information of the Hurricane Irma was obtained from the Atlantic hurricane
74 database (HURDAT2)[15], available online at the National Hurricane Center (NHC) of
75 the United States of America web page. This dataset is a re-analysis effort to extend and
76 revise the NHC's North Atlantic hurricane dataset (HURDAT).

77 The rain rate from the Global Precipitation Measurement (GPM) [16] was used. In
78 this dataset, the precipitation is estimated from the various precipitation-relevant
79 satellite passive microwave sensors comprising the GPM constellation, computed using
80 the Goddard Profiling Algorithm. This dataset is merged into half-hourly 0.1°x 0.1° of
81 latitude and longitude horizontal resolution.

82 *2.2 FLEXPART simulations*

83 Global outputs from a modeling experiment using the FLEXPART v9.0 [17] were
84 utilized to investigate the Hurricane Irma water budgets from 0000 UTC 30 August to
85 1200 UTC 13 September 2017. Initially, the model considers the atmosphere
86 homogeneously divided into approximately 2 million particles (the number of air
87 particles that must be higher than the meteorological model levels) uniformly
88 distributed over the entire globe and permits one to track them backward and/or
89 forward in time.

90 In this study, the particles residing over the area enclosed (target region) by the outer
91 radius of each Hurricane Irma best track position were tracked backward in time up to 10
92 days; which is considered the residence time of the water vapour in the atmosphere [18].

93 *2.3 Methodology*

94 *2.3.1 Lagrangian water budget formulation*

95 Following Stohl and James [12], the net change of the water vapour content of a
 96 particle is estimated as:

$$(e - p) = m \left(\frac{dq}{dt} \right) \quad (1)$$

97 where e and p are the rates of moisture increases and decreases along the trajectory, m is
 98 the mass of each particle assumed as constant and q is the specific humidity. Furthermore,
 99 to computed the surface freshwater flux over an area A , the moisture changes of all
 100 particles in the atmospheric column over A are computed as:

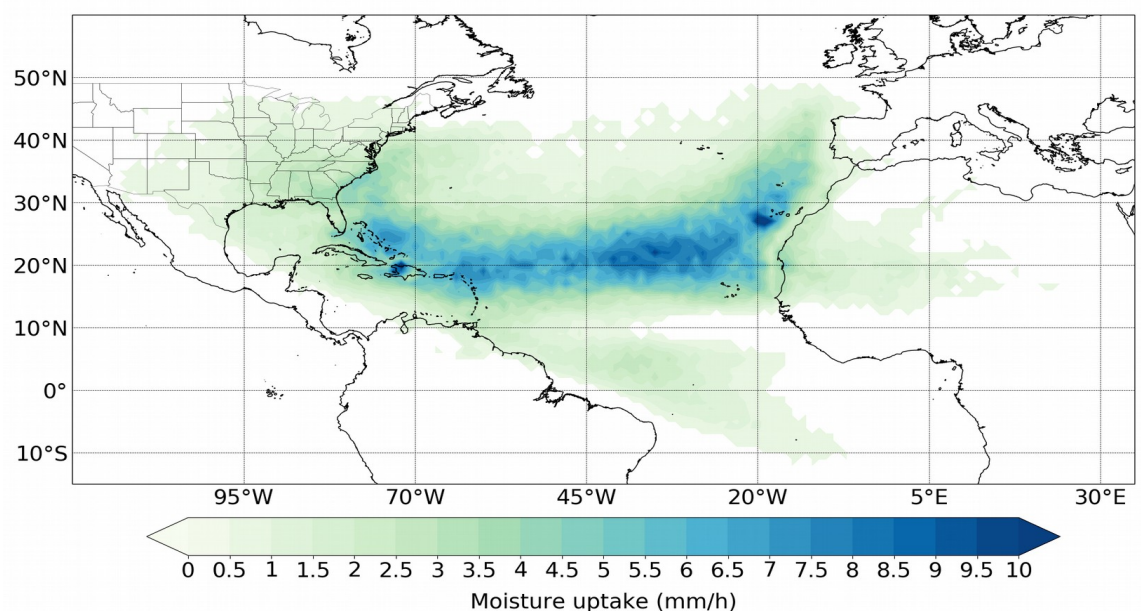
$$(E - P) = \frac{\sum_{k=1}^N (e - p)_k}{A} \quad (2)$$

101 where N is the number of particles residing over A . To identify the moisture source, the
 102 regions where the total evaporation (E) exceeds the total precipitation (P) should be
 103 selected, so only those regions showing $(E - P) > 0$ values are taken into account. We
 104 consider here that the moisture uptake ($E - P > 0$) is the net water vapour flux that arrived
 105 at the target region at each position every 6-h of the Hurricane Irma best track, and in its
 106 calculation is not included the precipitation over the target region.

107 3. Results and Discussion

108 3.1 Identification of the moisture sources for hurricane Irma genesis and intensification

109 The moisture uptake composite from 0000 UTC 30 August to 1200 UTC 13
 110 September reveals the moisture sources for hurricane Irma (2017) genesis and
 111 intensification. Clearly, from Figure 2 we identified the eastern North Atlantic along the
 112 northwest coast of Africa, from the Iberian Peninsula to the genesis position, and the
 113 Sahel region, as the main moisture sources that favored the activation of the convection
 114 when Irma was still a tropical disturbance embedded in an easterly wave [14]. The
 115 circulation of the North Atlantic Subtropical High-Pressure system (NASH) and the
 116 easterly winds acted as the moisture transport mechanisms from the source regions to
 117 the genesis location.



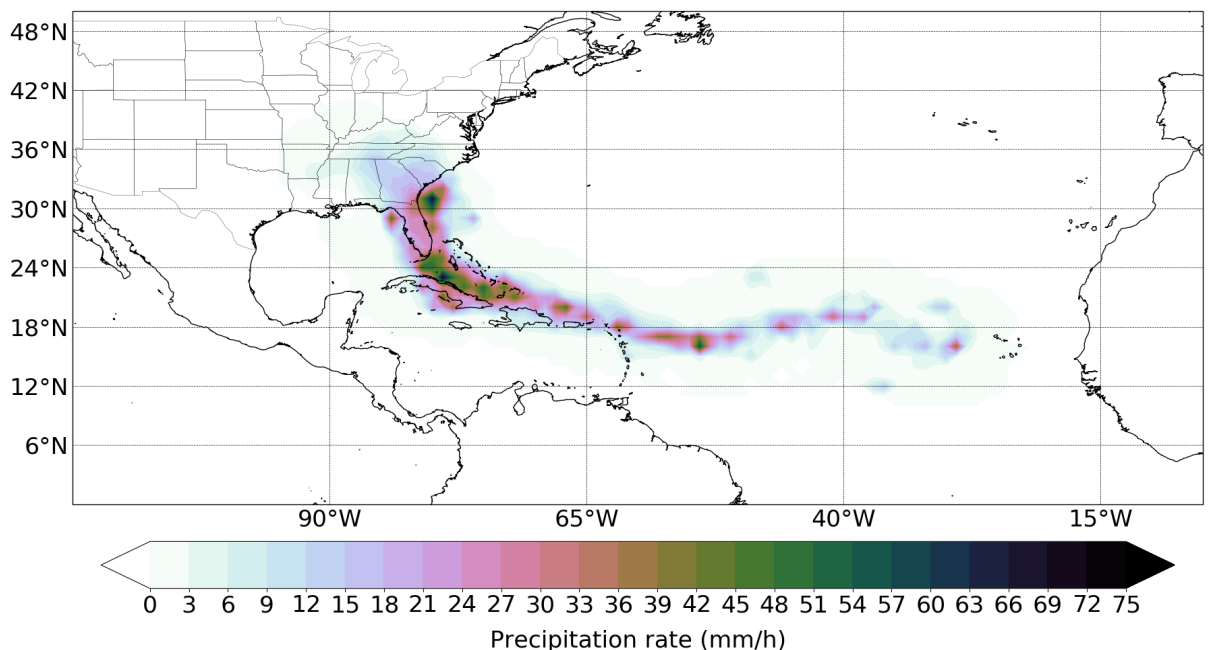
118
 119 **Figure 1.** Moisture uptake composite along the Hurricane Irma trajectory from 0000 UTC 30 August to 1200
 120 UTC 13 September.

121 Along the trajectory of Hurricane Irma, the easterly winds and the trade winds
 122 continued supplying atmospheric humidity to TC, which favored the intensification
 123 processes. Furthermore, the South Atlantic Subtropical High-Pressure system (SASH)
 124 transport water vapour from the South Atlantic Ocean to the Caribbean Sea, and then,
 125 the easterly winds move it towards Irma position. Additionally, the Caribbean Sea and
 126 the Gulf of Mexico contributed the atmospheric humidity required by Irma to keep the
 127 deep convection and warm core by releasing latent heat. Nevertheless, the band between
 128 15° and 30° North latitude over the Atlantic Ocean exhibits the greatest moisture
 129 contribution for Irma development. At the end of Irma's lifetime over the southeastern
 130 United States, we assume that a recycling process played an important role in moisture
 131 supplying. These findings are supported by the vertical integrated moisture flux pattern.
 132

133 3.2 Precipitation rate spatial distribution

134 Figure 2 shows the precipitation rate from GPM along the Hurricane Irma
 135 trajectory. Although Irma was already a major hurricane just 48 hours after the genesis,
 136 the intensity of the precipitation was less than 8 mm/h during the initial lifetime. This
 137 features may be linked to the fact that the inner core was quite compact at this time, with
 138 an estimated extension of 40 km [14].

139 After the hurricane reached its maximum intensity close to the islands at north of
 140 the Lesser Antilles Arc, the intensity of precipitation increased to be maximum higher
 141 than 36 mm/h during its movement along the North coast of Cuba, the Straits of Florida,
 142 and the Florida Peninsula, as shown in Figure 2. At this time, the most intense
 143 precipitation rates nuclei were located towards the northeast (NE) quadrant of the
 144 storm, coinciding with the regions with the highest moisture uptake, as can be easily
 145 verified in Figures 1 and 2.
 146

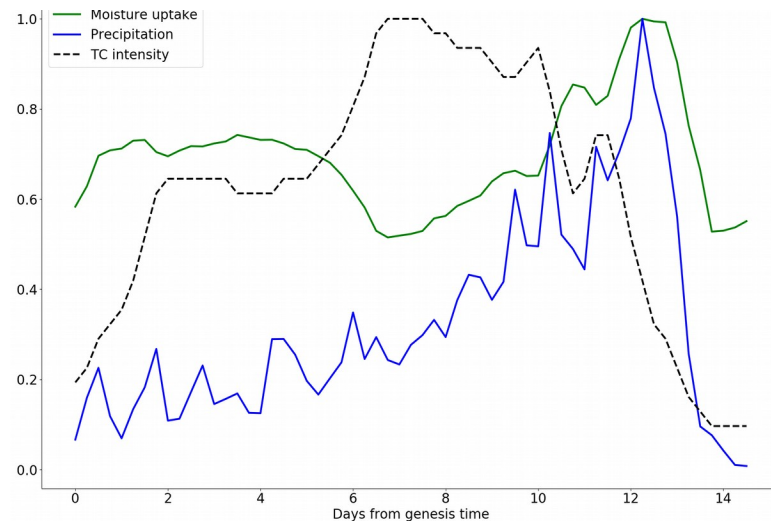


149 **Figure 2.** Rain rate from GPM composite along the Hurricane Irma trajectory from 0000 UTC 30 August to 1200
 150 UTC 13 September.

151 As Cangialosi et al. [14] pointed out, Irma produced very heavy rainfall across a
 152 central-eastern portion of Cuba and over the large portion of Florida Peninsula, the
 153 accumulated rainfall ranging from 250 to 380 mm.

154 3.3 Moisture uptake vs rain rate

155 From Figure 3 it can be inferred that in the 8 days after the Irma genesis, the
 156 moisture uptake was higher than the precipitation rate, which favored the continuous
 157 release of latent heat, a key factor in the intensification of TCs in agreement with
 158 Emanuel [19]. Nevertheless, in the last five days (from day 9 to day 14) of Irma as a TC,
 159 the moisture uptake and the rain rate temporal evolution is very similar, which
 160 corresponds to the high accumulated rainfall during its movement along the north coast
 161 of Cuba and the Florida Peninsula. It is notable that both magnitudes reach the
 162 maximum value at this time.
 163
 164
 165



166
 167 **Figure 3.** Normalized temporal evolution of moisture uptake from Lagrangian approach
 168 (green) and rain rate from GPM (blue) during hurricane Irma (2017) lifetime from 0000 UTC
 169 30 August to 1200 UTC 13 September. The gray dashed line represents the hurricane Irma
 170 intensity. The moisture uptake and rain rate plotted here represent the sum of all grid point
 171 within the area enclosed by the Hurricane Irma outer radius.
 172

173 Figure 4 reveals that Irma took most moisture from the environment no related to
 174 TC circulation than moisture from ocean evaporation within the area enclosed by
 175 the outer radius in each best track position. Therefore, the secondary circulation
 176 then transports more moisture inward and, thus, induces a stronger moist core. In
 177 other words, the strong radial inflow transports highly moist air parcels from the
 178 surrounding environment inward to the inner core.

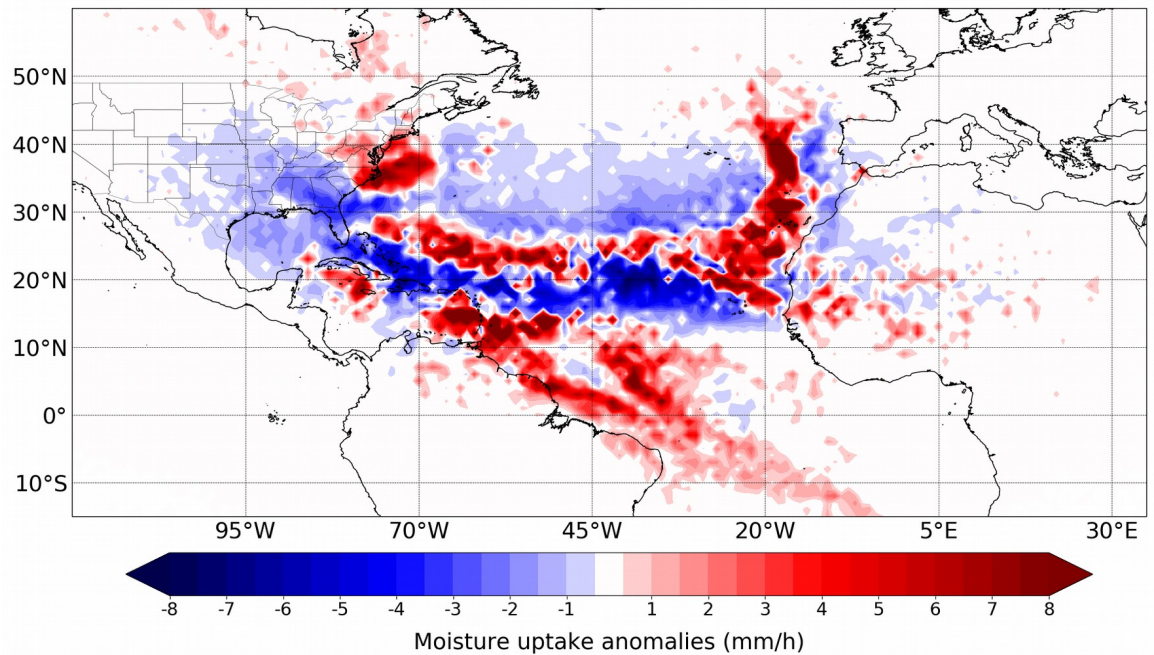


Figure 4. Accumulated moisture uptake anomalies (blue – red colors) along the Hurricane Irma trajectory from 0000 UTC 30 August to 1200 UTC 13 September. The moisture uptake anomalies were compute using the period 1980-2018.

4. Conclusions

In this study we performed the Hurricane Irma (2017) water budget analysis through a Lagrangian approach. The Hurricane Irma was one of the most severe hurricanes of the 2017 cyclonic season on the North Atlantic basin, and caused heavy rainfall along the north coast of Cuba and Florida Peninsula. To determine the moisture uptake for each position of the Irma best track and the water budget inside the system, the particle dispersion model FLEXPART.

The results showed that the North Atlantic Ocean between 15°-30° North latitude, the Sahel region, and the South Atlantic were the main moisture sources for the genesis and development of Irma. Although, the Caribbean Sea, the Gulf of Mexico, and the southeastern of United States of America also contributed, but to a lesser extent. Furthermore, the North Atlantic Subtropical High-Pressure system, the South Atlantic Subtropical High-Pressure system, and the easterly winds were identified as the main moisture transport mechanisms for supplying atmospheric humidity to Irma.

Despite the great intensity of Irma, during the first five-six days after genesis, the precipitation rate was less than 8 mm/h, however, when the hurricane center crossed over the Greater Antilles as an intense hurricane, the precipitation rate was greater than 20 mm/h, which supports the accumulated rainfall reported in Cuba and La Florida.

As expected, the moisture supplied from the surface under the area delimited by hurricane size is small, thus, the water vapour supplied from the environment through the secondary circulation transports more moisture inward. The accumulated moisture uptake anomalies along the hurricane Irma trajectory showed that both the Tropical North and South Atlantic Oceans were important sources of moisture for Irma development. However, the region of West Africa and the North Atlantic Ocean near the African continent and the Iberian Peninsula also provided humidity.

Author Contributions: A.P-A., R.N, and L.G. conceived the idea of the study. A.P-A., R.S., J.C.F-A. and P.C-H processed the data and made the figures. A.P-A. analyzed the results and wrote the manuscript. All authors analyzed the results and revised the final version of the manuscript.

Funding: The LAGRIMA project (grant no. RTI2018-095772-B-I00) was funded by the Ministerio de Ciencia, Innovación y Universidades, Spain. Partial support was also obtained from the Xunta de Galicia under the project “Programa de Consolidación e Estructuración de Unidades de Investigación Competitivas (Grupos de Referencia Competitiva)” (no. ED431C 2017/64-GRC).

Institutional Review Board Statement: Not applicable

Informed Consent Statement: Not applicable

Data Availability Statement: The datasets used in this study are freely available on internet. The HURDAT2 database is accessible from <https://www.nhc.noaa.gov/data/#hurdat>, and the GPM dataset is available at <https://gpm.nasa.gov/data/directory>. The FLEXPART outputs to reproduce our results is obtained upon request from the corresponding author.

Acknowledgments: A.P-A. acknowledges the support from UVigo PhD grants. J.C.F-A. and R.S. acknowledge the support from the Xunta de Galicia (Galician Regional Government) under the grants no. ED481A-2020/193 and ED481B 2019/070, respectively. We also thanks to Xunta de Galicia under Project ED431C 2017/64-GRC “Programa de Consolidación e Estructuración de Unidades de Investigación Competitivas (Grupos de Referencia Competitiva)”,co-funded by the European Regional Development Fund, European- Union (FEDER).

Conflicts of Interest: The authors declare no conflict of interest

References

1. Shultz, J. M.; Russell, J.; Espinel, Z. Epidemiology of Tropical Cyclones: The Dynamics of Disaster, Disease, and Development, *Epidemiol. Rev.* **2005**, *27*(1), 21–35, doi: 10.1093/epirev/mxi011
2. Gray WM. A global view of the origin of tropical disturbances and storms. *Mon. Wea. Rev.* **1968**, *96*, 669-700.
3. Emanuel KA. The dependence of hurricane intensity on climate. *Nature* **1987**, *326*,483–485.
4. Braun, S. A.; Sippel, J. A.; Nolan, D. S. The impact of dry mid-level air on hurricane intensity in idealized simulations with no mean flow, *J. Atmos. Sci* **2012**, *69*, 236–257, doi:10.1175/JAS-D-10-05007.1
5. Emanuel, K.; DesAutels, C.; Holloway, C.; Korty, R. Environmental control of tropical cyclone intensity, *J. Atmos. Sci.* **2004**, *61*, 843–858, doi:10.1175/1520-250469(2004)061<0843:ECOTCI>2.0.CO;2
6. Ge, X.; Li, T.; Peng, M. Effects of vertical shears and midlevel dry air on tropical cyclone developments, *J. Atmos. Sci.* **2013**, *70*, 3859–3875, doi:10.1175/JAS-D-13-066.1
7. Kimball, S. K. A modeling study of hurricane landfall in a dry environment, *Mon. Wea. Rev.* **2006**, *134*, 1901–1918, doi:10.1175/MWR3155.1
8. Wang, Z.; Montgomery, M. T.; Dunkerton, T. J. A dynamically-based method for forecasting 20 tropical cyclogenesis location in the Atlantic sector using global model products, *Geophys. Res. Lett.* **2009**, *36*, L03801, doi:10.1029/2008GL035586,
9. Tao, D.; Zhang, F. Effect of environmental shear, sea-surface temperature, and ambient moisture on the formation and predictability of tropical cyclones: an ensemble-mean perspective, *J. Adv. Model. Earth Syst.* **2014**, *6*, 384–404, doi:10.1002/2014MS000314
10. Ying, Y.; Zhang, Q. A modeling study on tropical cyclone structural changes in response to ambient moisture variations, *J. Meteor. Soc. Japan* **2012**, *90*, 755–770, doi:10.2151/jmsj.2012-512
11. Gimeno, L.; Stohl, A.; Trigo, R. M.; Dominguez, F.; Yoshimura, K.; Yu, L.; Drumond, A.; Durán-Quesada, A.M.; Nieto, R. Oceanic and Terrestrial Sources of Continental Precipitation, *Rev. Geophys.* **2012**, *50*, RG4003, doi:10.1029/2012RG000389.
12. Stohl, A.; James, P. A Lagrangian analysis of the atmospheric branch of the global water cycle. Part I: Method description, validation, and demonstration for the August 2002 flooding in central Europe. *J. Hydrometeorol.* **2004**, *5*, 656–678, doi: 10.1175/1525-7541(2004)005<0656:ALAOTA>2.0.CO;2
13. Stohl, A.; James, P. A Lagrangian analysis of the atmospheric branch of the global water cycle. Part II: Moisture transports between the Earth’s ocean basins and river catchments. *J. Hydrometeorol.* **2005** *6*, 961–984, doi: 10.1175/JHM470.1
14. Cangialosi, P. J.; Latta, S. S.; Berg, R. National Hurricane Center Tropical Cyclone Report. Hurricane Irma (AL112017). National Hurricane Center, 2018, https://www.nhc.noaa.gov/data/tcr/AL112017_Irma.pdf, Accessed on 14 March
15. Landsea, C. W.; Franklin, J. L. Atlantic Hurricane Database Uncertainty and Presentation of a New Database Format. *Mon. Wea. Rev.* **2013**, *141*, 3576–3592. doi: 10.1175/MWR-D-12-00254.1
16. Huffman, G.; Stocker, E.; Bolvin, D.; Nelkin, E.; Tan, J. GPM IMERG Early Precipitation L3 Half Hourly 0.1 degree x 0.1 degree V06, Green-belt, MD, Goddard Earth Sciences Data and Information Services Center (GES DISC), **2019**. doi:10.5067/GPM/IMERG/3B-HH-E/06. Accessed on 10 March 2021.
17. Stohl, A.; Forster, C.; Frank, A.; Seibert, P.; Wotawa, G. Technical note: The Lagrangian particle dispersion model FLEXPART version 6.2, *Atmos. Chem. Phys.* **2005**, *5*, 2461–2474, doi: 10.5194/acp-5-2461-2005

-
- 266 18. Numaguti, A. Origin and recycling processes of precipitating water over the Eurasian continent: Experiments using an
267 atmospheric general circulation model. *J. Geophys. Res.* **1999**, *104*, 1957–1972, doi: 10.1029/1998JD20002
- 268 19. Emanuel, K. A. An air–sea interaction theory for tropical cyclones. Part I: Steady-state maintenance. *J. Atmos. Sci.* **1986**, *43*,
269 585–604.